Biochimica et Biophysica Acta, 732 (1983) 266–275
Elsevier

BBA 71744

ELECTRON SPIN RESONANCE STUDIES ON THE INORGANIC-ANION-TRANSPORT SYSTEM OF THE HUMAN RED BLOOD CELL

BINDING OF A DISULFONATOSTILBENE SPIN LABEL (NDS-TEMPO) AND INHIBITION OF ANION TRANSPORT

K.F. SCHNELL, W. ELBE, J. KÄSBAUER and E. KAUFMANN

Institut für Physiologie der Universität Regensburg, Postfach 397, 8400 Regensburg 2 (F.R.G.)

(Received April 25th, 1983)

Key words: Anion transport inhibition; Spin label; ESR; (Erythrocyte membrane)

The disulfonatostilbene spin label, NDS-TEMPO, was synthesized (purity over 96%) and the binding of the spin label to human red-cell ghosts was studied. NDS-TEMPO is readily adsorbed to the membrane surface. Both pretreatment of the ghosts with FDNB and DIDS and the presence of DNDS completely prevent the binding of NDS-TEMPO to red-cell ghosts. Chloride and sulfate competitively inhibit the binding of NDS-TEMPO. Conversely, NDS-TEMPO is a strong, competitive inhibitor of chloride and of sulfate transport. The dissociation constants of NDS-TEMPO from the ESR studies were in the range 1.0–2.0 μM (pH 7.6, 20°C). The inhibition constants of NDS-TEMPO as obtained from the flux experiments were in the range 0.5–2.5 μM (pH 7.3, 25°C). The close accordance of the NDS-TEMPO dissociation constants from the ESR studies with the NDS-TEMPO inhibition constants from the flux measurements indicate a specific labeling of the inorganic-anion-transport system.

Introduction

The transport of inorganic anions across the red-cell membrane is mediated by a specific anion-transport system [1–3]. Disulfonatostilbene derivatives such as SITS, DIDS, H_2-DIDS, DNDS and DBDS are strong, specific inhibitors of the anion transport in red cells and have proven to be useful tools in transport research. SITS, DIDS and H_2-DIDS bind covalently to the inorganic-anion-transport system and have been used for the identification of the anion-transport protein, band 3. H_2-DIDS has been employed to determine the number of anion-binding sites per cell [4–11]. DNDS, DBDS and H_2-DIDS at low temperature are reversible competitive inhibitors of the anion transport in red cells [12–17]. They have been used to characterize the outward-facing anion-binding site of the anion transporter. The equilibrium binding of DNDS and of DBDS to the red cell membrane has been measured by ultraviolet/visible spectroscopy and by fluorescence spectros-

Abbreviations: ANDS, 4-amino-4′-nitro-2,2′-stilbenedisulfonic acid, K salt; BNDS, 4-benzamido-4′-nitro-2,2′-stilbenedisulfonic acid; DADS, 4,4′-diamino-2,2′-stilbenedisulfonic acid, Na salt; DBDS, 4,4′-dibenzoamide-2,2′-stilbenedisulfonic acid, K salt; DIDS, 4,4′-diisothiocyanato-2,2′-stilbenedisulfonic acid, Na salt; DNDS, 4,4′-dinitro-2,2′-stilbenedisulfonic acid, Na salt; FDNB, 1-fluoro-2,4-dinitrobenzene; INDS, 4-isothiocyanato-4′-nitro-2,2′-stilbenedisulfonic acid, K salt; MAL-TEMPO, *N*-4-maleimido-2,2,6,6-tetramethylpiperidine-1-oxyl; NCS-TEMPO, 4-isothiocyanato-2,2,6,6-tetramethylpiperidine-1-oxyl; NDS-TEMPO, *N*-4-(2,2,6,6-tetramethyl-1-oxyl)piperidinyl-*N*′-4-(4′-nitro-2,2′-stilbenedisulfonic acid) thiourea, K salt; NH_2-TEMPO, 4-amino-2,2,6,6-tetramethylpiperidine-1-oxyl; SITS, 4-acetamido-4-isothiocyamato-2,2′-stilbenedisulfonic acid.

copy [13–17]. In addition, equilibrium binding studies have been performed with radioactively labeled DNDS [17] and BNDS (1982, unpublished data). To date, no attempt has been made to label the inorganic anion-transport system of the red cell with specific spin probes. This is due mainly to the lack of appropriate spin labels which exhibit a high specificity and a high affinity for the inorganic-anion-transport system.

Nitroxide spin labels are well suited for equilibrium binding studies and for the study of slow or stationary conformational changes. ESR spectroscopy offers some advantages over other spectroscopic techniques and appears to be supplementary to NMR, ultraviolet/visible and fluorescence spectroscopy. For details see Ref. 18. In general, ESR spectroscopy has a much higher sensitivity than NMR spectroscopy. Biological membranes usually have no intrinsic paramagnetic groups that could interfere with the ESR spectroscopy of nitroxide spin labels. ESR spectroscopy is insensitive to light scattering, quenching, background absorption and background fluorescence: effects which may raise serious problems in ultraviolet/visible and fluorescence spectroscopy. Thus, ESR spectra can be recorded from concentrated cell suspensions. Furthermore, the intracellular concentration of free and bound spin label can be measured without disrupting the cells. For instance, once it is possible to synthesize non-penetrating spin labels, the binding of the label to the inner membrane surface of red cells can be assessed by trapping the spin probe within red-cell ghosts. On the other hand, the time resolution of ESR spectroscopy as compared to fluorescence spectroscopy is very low and nitroxide spin labels can be inactivated by reducing or oxidizing agents.

Nitroxide spin labels have been employed so far to study the polarity profile, the mobility of spin-labeled fatty acids and the protein-lipid interaction in biological membranes. In addition, spin probes have been used to investigate conformational changes and active site geometry in enzymes [19–23]. Recently, conformational changes of purified band 3 vesicles have been reported by labeling them with MAL-TEMPO [24]. In red-cell ghosts, MAL-TEMPO did not show any specificity for the inorganic-anion-transport system [25,26].

This paper is concerned with the synthesis of the disulfonatostilbene spin label, NDS-TEMPO. The binding of NDS-TEMPO to red-cell ghosts and its effect upon anion transport have been studied. NDS-TEMPO is a reversible, competitive inhibitor of the anion transport in red-cell ghosts. Concomitantly, the substrate anions, chloride and sulfate, are competitive inhibitors of NDS-TEMPO binding. NDS-TEMPO displays a high specificity for the inorganic anion transport system and is suited for studies of equilibrium binding in resealed ghosts of red cells. To date, these results have been published only in part [27,28].

Materials and Methods

Synthesis of NDS-TEMPO

For purification, ANDS was dissolved in hot water and precipitated by the addition of K_2CO_3. The product was dried in a desiccator over $CaCl_2$. 2.4 g of purified ANDS (5 mmol) were dissolved in 20 ml water. In order to convert ANDS to INDS, the ANDS solution was added in drops over a period of 30 min to a well-stirred thiophosgene/water solution (1 ml $CSCl_2$ (13 mmol)/25 ml water, 0°C) and the reaction was allowed to continue for another 45 min. The product was crystallized at 0°C by the addition of K_2CO_3. The precipitate was filtered by suction, carefully washed with diethyl ether and evaporated. For further purification, the residue was extracted by methanol, the extract was filtered and the solvent was removed by subsequent evaporation. The residue was dried in a desiccator over $CaCl_2$ and consisted of light-yellow, microcrystalline INDS. The yield of INDS was 1.94 g (3.7 mmol, 74% of the theoretical amount).

NDS-TEMPO was synthesized by reacting INDS with NH_2-TEMPO. 500 mg INDS (0.9 mmol) were dissolved in 3 ml water and reacted in the dark with 200 mg (1.2 mmol) NH_2-TEMPO at 0°C. After 30 min, the excess NH_2-TEMPO was removed by extraction with diethyl ether. The product was isolated by freeze-drying ($1 \cdot 10^{-2}$ Torr, −180°C) and purified by extraction with absolute ethanol. The yield was 350 mg (0.5 mmol, 56% of the theoretical amount). The purity of the compound as checked by HPLC was found to be greater than 96% (HPLC, Hewlett Packard 1080, Column RP-8, 10 μm, diameter 3 mm, 25 cm;

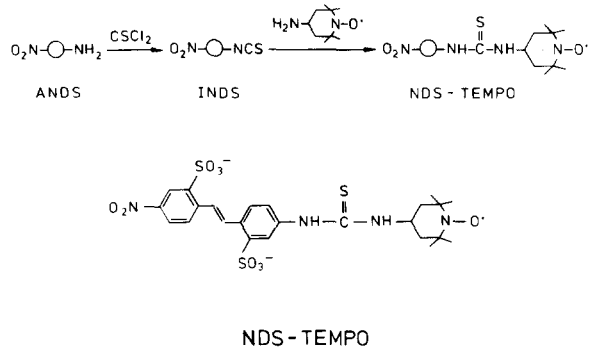

Fig. 1. Synthesis and structure of NDS-TEMPO. For details see text. The open circles denote the 2,2'-disulfonatostilbene moiety of the molecules.

mobile phase: 5 mM tetrabutylammonium phosphate in water/methanol (55 : 45)). ANDS, INDS, DADS and NH_2-TEMPO can easily be separated from NDS-TEMPO by analytic HPLC. The structure of NDS-TEMPO was confirmed by elementary analysis, infrared spectroscopy and ESR spectroscopy of NDS-TEMPO and other disulfonatostilbene derivatives. The molecular weight of NDS-TEMPO · 3 H_2O, K salt is 743. NDS-TEMPO is stable in water. The ESR activity of NDS-TEMPO, stored at −20°C in the dark, was stable for at least 3 months. The synthesis and structure of NDS-TEMPO are shown in Fig. 1.

Preparation of the red-cell ghosts

Red-cell ghosts were prepared as follows [29–31]. Fresh human red cells were washed three times in 10 vol. of an isotonic, 122 mM potassium citrate solution (20°C, pH 7.3). Plasma and leukocytes were removed. 1 g tightly packed, sedimented red cells (centrifugation 5000 × *g*, 10 min) were added to 1 ml 122 mM potassium citrate solution to make a 50% (w/v) cell suspension. The suspension was cooled to 0°C. The red cells then were hemolysed at 0°C, pH 6.2. For this purpose, 10 vol. of an ice-cold hypotonic 4 mM $MgSO_4$/3.8 mM CH_3COOH solution were added to 1 vol. of cell suspension and the suspension was stirred for 5 min. Thereafter, isotonicity was restored by adding hypertonic potassium citrate/Tris/KCl or potassium citrate/Tris/K_2SO_4 solutions (0°C, pH 7.3). The final composition of the resealing solutions was 40 mM potassium citrate, 40 mM Tris and up to 150 mM KCl or 100 mM K_2SO_4. Isoosmotic substitution was made either with sorbitol or with potassium citrate. The resealing of the red-cell ghosts was achieved by incubating them for 45 min at 37°C, pH 7.3. After resealing, the ghosts were washed twice in 20 vol. of the same solution. Approx. 90% of the red-cell ghosts regain a low permeability to potassium and [^{3}H]sucrose.

ESR spectra

The equilibrium binding studies of NDS-TEMPO to red-cell ghosts were performed with 50% ghost suspension if not stated otherwise. Resealed ghosts from 1.0 g red cells were suspended in 1 ml of the respective resealing solution. The number of ghosts per ml suspension was checked by counting the ghosts with a Coulter Counter, model DN. To the ghost suspension and to the reference solutions were added distinct amounts of NDS-TEMPO. The ESR spectra were recorded with a Varian ESR spectrometer. Samples of 70 µl each were added into calibrated microhematocrit tubes and placed into the cavity of the ESR spectrometer. NDS-TEMPO is stable in water. The ESR spectra of NDS-TEMPO dissolved in KCl, K_2SO_4, potassium citrate and potassium citrate/Tris/sorbitol solutions of different concentrations remained unchanged over a period of several hours. In 40 mM potassium citrate/40 mM Tris/220 mM sorbitol solutions (20°C, pH 6.9) the ESR spectrum of NDS-TEMPO was stable for at least 10 h. Tests with 50% ghost suspensions in 40 mM potassium citrate/40 mM Tris/220 mM sorbitol and 40 mM potassium citrate/40 mM Tris/150 mM KCl have shown that the ESR activity of NDS-TEMPO remains stable over a period of about 60 min (25°C, pH 7.3). Upon addition of 1 mM DNDS, a complete recovery of the mobile ESR signal was obtained (compare Fig. 2). Microwave power, modulation amplitude, modulation frequency, scan range, scan time, filter time constant and receiver gain setting are indicated in the legends of the figures. Due to the high dielectric loss caused by water, a high microwave power was required for the measurements. Care was taken to avoid distortions of the ESR spectra which could result from saturation effects or inappropriate choice of the scan time and of the filter time constant.

The concentration of free NDS-TEMPO was determined from the line height of the sharp low-field or the sharp high-field line of the ESR spectra [18,32]. Calibration curves of NDS-TEMPO in isotonic (330 mosM) or double isotonic solutions (660 mosM) of KCl, K_2SO_4, potassium citrate and potassium citrate/Tris/sorbitol exhibited a linear relation between line height and NDS-TEMPO concentration over a range 0.5–50 μM. The salt composition of the solutions had no effect upon shape and line height of the ESR signal; in double isotonic solutions the line-height of the ESR signal was approx. 2% lower than in isotonic solutions.

The amount of bound NDS-TEMPO was calculated from the concentration of free NDS-TEMPO before and after the addition of 1 mM DNDS to the ghost suspensions. DNDS causes a complete release of bound NDS-TEMPO from the membrane surface without interfering with the ESR spectroscopy (compare Fig. 2). As far as our experiments are concerned no corrections of the line height of the sharp ESR signal for the underlying broad ESR signal were necessary. The equilibrium concentration of free NDS-TEMPO of the ghost suspension was measured after removing the ghosts by centrifugation (50 000 × g, 10 min, 20°C) or was calculated from the line height of the sharp low-field line and the hematocrit of the ghost suspension. The analysis of the equilibrium binding data of NDS-TEMPO is shown in Fig. 4. For details of the plotting procedures see Refs. 33,34,3,14,17.

Flux measurements

The unidirectional fluxes of chloride and of sulfate were determined under self-exchange conditions [35,36]. The tracer efflux from radioactively labeled resealed ghosts into a non-radioactive solutions was measured. The back-exchange solutions had the same salt composition as the respective resealing solutions. In addition, they contained increasing concentrations of NDS-TEMPO (1–20 μM).

The chloride flux experiments were executed with 1% ghost suspension ($1.11 \cdot 10^8$ ghosts/ml suspension) at 0°C, pH 7.3, by using a filtration techniques [37]. The sulfate flux experiments were carried out with 10% ghost suspension ($1.11 \cdot 10^9$ ghosts/ml suspension) at 25°C, pH 7.3, by means of a centrifugation technique. All fluxes are expressed in mol/min per g cells, where the term 'g cells' refers to the wet weight of tightly packed red cells. For details see Ref. 38.

The equilibrium concentration of free NDS-TEMPO in ghost suspensions was determined from the height of the sharp low-field signal as outlined above. For analysis of the flux experiments in the presence of NDS-TEMPO Dixon plots were used as shown in Fig. 5. Concerning details of the plotting procedures, see Refs. 33, 34, 2, 3, 12.

Chemicals

ANDS was a gift from Bayer AG., Leverkusen, F.R.G. DNDS was purchased from ICN Pharmaceuticals, Plainview, NY, U.S.A. DIDS was synthesized by the method of Cabantchik and Rothstein [6]. NH_2-TEMPO was purchased from EGA-Chemie, Steinheim/Albuch, F.R.G. FDNB G.R., sorbitol, Tris and bovine serum albumin were purchased from Serva, Heidelberg, F.R.G. KCl, K_2SO_4 of G.R. grade and potassium citrate, pure, were from Merck, Darmstadt, F.R.G.

Results

Fig. 2 shows the binding of NDS-TEMPO to red-cell ghosts. The ESR spectra were recorded from a 80% ghost suspension in isotonic potassium citrate/Tris/sorbitol. To all samples was added 10 μM NDS-TEMPO. Trace 'a' exhibits the ESR spectrum of NDS-TEMPO dissolved in potassium citrate/Tris/sorbitol. The three sharp line signal is indicative of free mobility of NDS-TEMPO. Trace 'b' shows the adsorption of NDS-TEMPO to red-cell ghosts. A composite ESR spectrum is obtained. The height of the sharp ESR lines is reduced and a broad signal in the low-field region emerges which indicates the immobilization of NDS-TEMPO. 500 mM KCl causes a partial release of bound NDS-TEMPO (trace 'c'). As compared to trace b, the height of the sharp lines is increased and the broad line in the low-field region has disappeared. However, the chloride concentration was not sufficiently high to release the bound NDS-TEMPO completely. The addition of 1 mM DNDS results in a complete recovery of the sharp ESR signal (compare traces a and d). Potassium sulfate exerts effects upon the release of

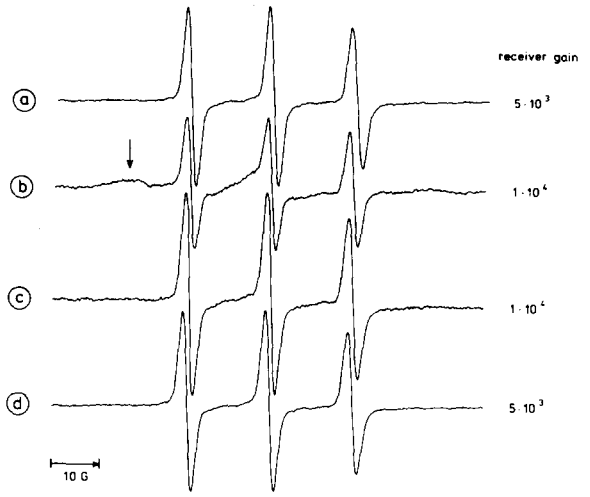

Fig. 2. Binding of NDS-TEMPO to red-cell ghosts. (a) ESR spectrum of NDS-TEMPO dissolved in sorbitol/Tris/potassium citrate solution. (b) ESR spectrum of NDS-TEMPO from a suspension of ghosts. The broad signal in the low field region is marked by an arrow. (c) ESR spectrum of NDS-TEMPO from the same suspension of ghosts upon the addition of 500 mM KCl. (d) ESR spectrum of NDS-TEMPO from the same suspension of ghosts after the addition of 1 mM DNDS. All samples contain 10 μM NDS-TEMPO. The experiments were conducted with an 80% ghost suspension containing $8.9 \cdot 10^9$ ghosts/ml suspension. The ghosts were resealed and resuspended in isotonic 40 mM potassium citrate/40 mM Tris/220 mM sorbitol. Osmolarity, 330 mosM. The ESR spectra were recorded at 20°C pH 7.6. Field set, 3400 G; microwave power, 50 mW; frequency, 9.5 GHz; modulation amplitude, 2.5 G; modulation frequency, 100 kHz; scan time, 8 min; filter time constant, 1 s; receiver gain setting as indicated at the respective traces.

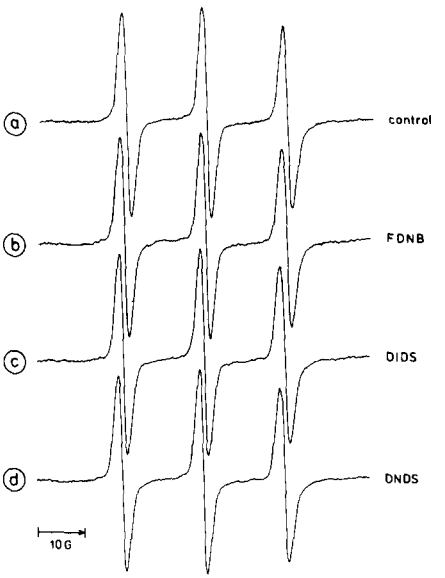

Fig. 3. Effect of FDNB, DIDS and DNDS upon the binding of NDS-TEMPO to red-cell ghosts. (a) ESR spectrum of NDS-TEMPO dissolved in 40 mM potassium citrate/220 mM sorbitol. (b) ESR spectrum of NDS-TEMPO from a 50% suspension of FDNB-treated red-cell ghosts. (c) ESR spectrum of NDS-TEMPO from a 50% suspension of DIDS-treated red-cell ghosts. (d) ESR spectrum of NDS-TEMPO from a 50% ghost suspension in the presence of 1 mM DNDS. To each sample 5 μM NDS-TEMPO were added. The red-cell ghosts were prepared and suspended in an isotonic 220 mM sorbitol/40 mM potassium citrate solution. After resealing, a 10% ghost suspension was made, samples (b) and (c) were treated with 2 mM FDNB or 2 mM DIDS (45 min, 37°C, pH 7.6). Subsequently, the ghosts were washed twice in 20 vol. of the same potassium citrate/sorbitol solution. To sample (d) 1 mM DNDS was added. The ESR spectra were recorded at 20°C (pH 7.6) from 50% ghost suspensions containing $5.56 \cdot 10^9$ ghosts/ml suspension. Field set, 3400 G; modulation amplitude, 2.5 G; frequency, 9.5 GHz; microwave power, 50 mW; scan range, 100 G; scan time, 16 min; filter time constant, 3 s; receiver gain setting, $5 \cdot 10^3$.

NDS-TEMPO similar to those of KCl. Under our experimental conditions, no uptake of NDS-TEMPO by red-cell ghosts was observed.

In order to test the specificity of NDS-TEMPO for the inorganic-anion-transport system, the transport system was blocked by specific inhibitors of the anion transport. FDNB and DIDS are irreversible inhibitors which bind covalently to band 3 [5–8,39,40]. DNDS, ANDS and BNDS are reversible competitive inhibitors of the anion transport in red cells [2,3,12–17]. According to our studies, the doses employed were sufficiently high to cause a more than 98% inhibition of the sulfate and of the chloride transport. As shown in Fig. 3, pretreatment of red-cell ghosts with FDNB or DIDS prevents the binding of NDS-TEMPO. Also, high concentrations of DNDS, ANDS and BNDS (ANDS and BNDS are not shown) completely inhibit the binding of NDS-TEMPO to red-cell ghosts. Substrate anions such as chloride, bicarbonate, nitrate and sulfate inhibit the binding of NDS-TEMPO to red-cell ghosts. In order to identify the mechanism of inhibition, the concentration dependence of NDS-TEMPO binding to red-cell ghosts in the presence of substrate anions was studied. The ghosts were resealed and suspended in solutions of fixed substrate anion

concentrations. The concentrations of free and of bound NDS-TEMPO were determined by the line height of the sharp ESR signal (see Materials and Methods section). All experiments were executed under self-exchange conditions.

The results of the equilibrium-binding studies are shown in Fig. 4. The Klotz plots (double-reciprocal plots) are bound vs. free NDS-TEMPO were linear over a range of 0.5–10 μM NDS-TEMPO. At concentrations above 20 μM, systematic deviations became apparent which we have not yet pursued in detail. Citrate has no effect upon NDS-TEMPO binding. In contrast to citrate, chloride and sulfate inhibit competitively the binding of NDS-TEMPO to red-cell ghosts. In the presence of chloride or of sulfate, the double-reciprocal plots increase in slope but the $1/L_B$ axis intercept remains constant. The slope replot of a family of Klotz plots vs. chloride concentration is shown in Fig. 4b. The replots of slope vs. chloride concentration were linear up to approx. 100 mM, pointing to a pure competitive inhibition of NDS-TEMPO binding. Corresponding results were obtained with bicarbonate, nitrate and sulfate. The maximal binding capacity of the suspension for NDS-TEMPO and the apparent NDS-TEMPO dissociation constants were obtained from the intersection of the straight lines with the $1/L_B$ and the $1/[L_f]$ axis, respectively. The dissociation constants of NDS-TEMPO and of the substrate anion were determined by replots of $K_{L(app)}$ vs. substrate anion concentration (Fig. 4c).

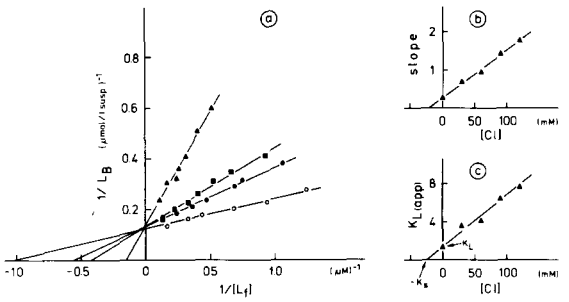

Fig. 4. Equilibrium binding of NDS-TEMPO to red-cell ghosts. (a) Klotz plot. Ordinate: Reciprocal amount of bound NDS-TEMPO, $1/[L_B]$ (μmol/l suspension)$^{-1}$. Abscissa: Reciprocal concentration of free NDS-TEMPO, $1/[L_f]$ (μM^{-1}). The ghosts were resealed and resuspended in isotonic solutions (330 mosM) of 40 mM potassium citrate/40 mM Tris/220 mM sorbitol (●), 112 mM potassium citrate/40 mM Tris (○), 40 mM potassium citrate/40 mM Tris/110 mM (▲) and 40 mM potassium citrate/40 mM Tris/80 mM K_2SO_4 (■). (b) Replot of slope vs. [Cl]. (c) Replot of $K_{L(app)}$ vs. [Cl]. All experiments were executed with 50% ghost suspensions, i.e., $5.56 \cdot 10^9$ ghosts/ml suspension. Isoosmotic substitution was made with 122 mM potassium citrate solution. The suspensions were subdivided into 6–8 samples of 2 ml. 2–30 μM NDS-TEMPO was added to the samples. The concentrations of bound and of free NDS-TEMPO were determined as outlined in the method section. The ESR spectra were recorded at 20°C (pH 7.6) as indicated in the legend to Fig. 2. Plotting procedures were as follows. For a single class of binding sites and a competitive inhibition of NDS-TEMPO binding by the substrate anion, S, the inverted adsorption isotherm for NDS-TEMPO reads:
$1/L_B = K_L(1+[S]/K_s)/L_{Bmax}[L_f]+1/L_{Bmax}$
slope $= K_L(1+[S]/K_s)/L_{Bmax}$, $K_{L(app)} = K_L(1+[S]/K_s)$
K_L and K_s are the dissociation constants of NDS-TEMPO and of the substrate anion, S; $K_{L(app)}$ is the apparent NDS-TEMPO dissociation constant and L_{Bmax} the maximal binding capacity of the suspension. The $1/L_B$ intercept is $1/L_{Bmax}$, the $1/[L_f]$ intercept is $-1/K_{L(app)}$.

The dissociation constants of NDS-TEMPO and of some substrate anions and the average number of NDS-TEMPO binding sites per cell are listed in Table I. The NDS-TEMPO dissociation constant is of the same order of magnitude as the dissociation constants of DNDS and DBDS [2,3,12–17]. The number of NDS-TEMPO binding sites per cell is consistent with the number of disulfonatostilbene binding sites reported in the literature [6,8,13,14,17].

NDS-TEMPO is a strong reversible inhibitor of the anion transport in red-cell ghosts. Fig. 5 exhibits the action of NDS-TEMPO on sulfate transport. Up to 20 μM NDS-TEMPO, the Dixon plots were linear and always displayed a competitive type of inhibition (Fig. 5a). The slope replots of the Dixon plots were linear and passed through the origin (Fig. 5b). Similar results were obtained when the chloride flux in red-cell ghosts was studied. The Dixon plots together with the slope replots provide strong evidence for a pure competitive inhibition and rule out a mixed-type inhibition. The inhibition constants of NDS-TEMPO and the half-saturation constants of the substrate anions can best be determined by replots of the apparent NDS-TEMPO inhibition constant vs. the substrate anion concentration (Fig. 5c) [2,3,12,14,17]. The apparent inhibition constant of NDS-TEMPO is obtained from the intersection of the straight lines with the $[L_f]$ axis as shown in Fig. 5a.

TABLE I

BINDING OF NDS-TEMPO TO RED-CELL GHOSTS

K_L and K_s are the dissociation constants of NDS-TEMPO and of substrate anions (mean ± S.D., 3–4 experiments), [S] is the substrate anion concentration. 50% ghost suspension = $(5.56 \pm 0.13) \cdot 10^9$ ghosts/ml suspension (mean ± S.D., 22 experiments). Maximal NDS-TEMPO binding $L_{Bmax} = 8.10 \pm 0.71$ nmol/ml suspension. In addition to the main constituent, S, all solutions contain 40 mM potassium citrate and 40 mM Tris. Isoosmotic substitution was made with 122 mM potassium citrate: 330 mosM, pH 7.6, 20°C. K_L, K_s and L_{Bmax} were obtained from the Klotz plots as shown in Fig. 4. For sorbitol and potassium citrate K_L was set equal to $K_{L(app)}$.

Solution	[S] (mM)	K_L (μM)	K_s (mM)
Sorbitol	220	1.79 ± 0.14	–
Potassium citrate	122	1.05 ± 0.10	–
Potassium chloride	0–120	1.23 ± 0.25	30 ± 5
Potassium sulfate	0– 80	1.60 ± 0.31	60 ± 12
Potassium bicarbonate	0– 60	1.29 ± 0.28	16 ± 4
Potassium nitrate	0– 60	1.24 ± 0.32	7 ± 2

NDS-TEMPO/cell: $(8.75 \pm 0.81) \cdot 10^5$, mean ± S.D., 22 experiments.

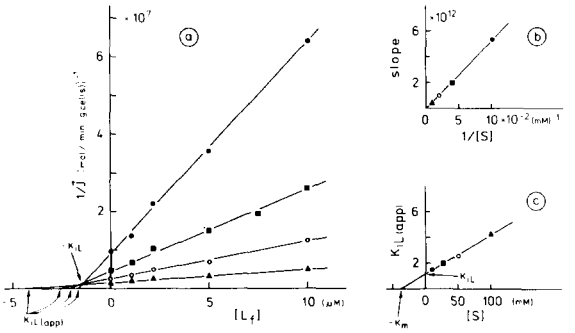

Fig. 5. Inhibition of the unidirectional sulfate flux by NDS-TEMPO, (a) Dixon plot. Ordinate: Reciprocal unidirectional sulfate flux, $1/\vec{J}$ (mol/min per g cells). Abscissa: Concentration of NDS-TEMPO, $[L_f]$ (μM). The sulfate concentration, [S], is indicated thus (mM): 10, ●; 25, ■; 50, ○; 100, ▲. The data were fitted by linear regression. (b) Replot of slope vs. 1/[S]. (c) Replots of $K_{iL(app)}$ vs. [S]. The sulfate flux experiments were conducted with a 10% ghost suspension at 25°C, pH 7.2. Isoosmotic substitution was made either with a 122 mM potassium citrate or with a 330 mM sorbitol solution. All solutions contain 40 mM potassium citrate, which is essential for the resealing of the ghosts. The plotting procedure was as follows. Under self-exchange conditions, the reciprocal flux equation for the unidirectional flux, $\vec{J}$, of the substrate anion, S, reads (the interaction of S with the modifier site having been neglected):

$1/\vec{J} = K_m(1 + [L_f]/K_{iL})/\vec{J}_{max}[S] + 1/\vec{J}_{max}$

slope $= K_m/(\vec{J}_{max}[S]K_{iL})$, $K_{iL(app)} = K_{iL}(1 + [S]/K_m)$

K_m and K_{iL} are the half-saturation constant of the substrate anion and the NDS-TEMPO inhibitor constant. $\vec{J}_{max}$ is the maximal unidirectional flux of S, and $K_{iL(app)}$ is the apparent NDS-TEMPO inhibitor constant. $K_{iL(app)}$ is obtained from the intersections of the straight lines with the $[L_f]$ axis. The replots of $K_{iL(app)}$ vs. [S] give K_{iL} and K_m.

The inhibition constants and the half-saturation constants of sulfate and chloride are summarized in Table II. The NDS-TEMPO inhibition constants are compatible with the inhibition constants of other strong, reversibly binding disulfonatostilbene inhibitors [2,3,12–17]. The half-saturation constants of chloride and of sulfate are in accordance with the half-saturation constants of the chloride and the sulfate self-exchange in red cells and red-cell ghosts as reported in the literature [3,31,38,40–47].

TABLE II

DIXON PLOT PARAMETER

K_{iL} is the inhibition constant of NDS-TEMPO; K_m is the half-saturation constant of the substrate anion, S. K_{iL} and K_m were determined from the replots of $K_{iL(app)}$ vs. [S] was shown in Fig. 5. Mean ± S.D., three experiments. Isoosmotic substitution was made with potassium citrate (122 mM) or with 220 mM sorbitol/40 mM potassium citrate. The chloride flux experiments were performed with a 1% ghost suspension, the sulfate flux experiments with a 10% ghost suspension.

Solution	K_{iL} (μM)	K_m (mM)
Chloride (pH 7.3, 0°C)		
potassium citrate substitution	0.42 ± 0.03	25.0 ± 5.3
Sulfate (pH 7.3, 25°C)		
potassium citrate substitution	1.83 ± 0.61	37.7 ± 6.4
Sulfate (pH 7.3, 25°C)		
sorbitol substitution	2.55 ± 0.63	44.2 ± 4.8

Discussion

Recognition of the importance of ESR spectroscopy in membrane biology has been growing in recent years. As was mentioned already, nitroxide spin labels have been employed to study the polarity profile of hydrophobic membrane domains, to investigate protein-lipid interactions and to monitor conformational changes in enzymes. Data on specific labeling of transport systems are rare, mainly for the want of appropriate spin labels [18–23]. Spin labels such as MAL-TEMPO and NCS-TEMPO are unspecific and can only be applied to purified or partial purified transport systems. Ginsburg et al. [24] have observed conformational changes in partial purified band 3 vesicles labeled with MAL-TEMPO. The conformational changes seem to be related to the transport function of band 3. We found that labeling red-cell ghosts with MAL-TEMPO or with NCS-TEMPO yielded strong, composite ESR spectra. However, we were unable to observe either an inhibition of the anion transport or conformational changes of band 3. The addition of SITS or DIDS did not inhibit the binding of NCS-TEMPO to red-cell ghosts [25,26]. These results demonstrate that MAL-TEMPO and NCS-TEMPO are not suited to labeling the inorganic anion transport system in intact red-cell membranes.

The present paper constitutes the first report on spin labeling of the inorganic-anion-transport system of the red cell with a specific disulfonatostilbene spin label, NDS-TEMPO. In spite of the introduction of the comparatively large NH_2-TEMPO moiety, NDS-TEMPO behaves like other disulfonatostilbene derivatives studied so far [2,3,12–17]. NDS-TEMPO is adsorbed to red-cell ghosts. The binding of NDS-TEMPO to the red-cell membrane is blocked by specific inhibitors of the anion transport. Substrate anions such as chloride, bicarbonate, nitrate and sulfate inhibit competitively the binding of NDS-TEMPO. Simultaneously, NDS-TEMPO acts as a reversible, competitive inhibitor of the chloride and the sulfate transport (Figs. 2–4). These results demonstrate the high specificity of NDS-TEMPO for the inorganic-anion-transport system. Our data do not give conclusive information on whether the mutual competition between NDS-TEMPO and substrate anion binding is steric or allosteric. Recent experiments have shown that competitive inhibitors of the anion transport such as salicylate coincidentally induce a competitive inhibition of NDS-TEMPO binding, while noncompetitive inhibitors such as phlorizin cause a noncompetitive inhibition of NDS-TEMPO binding. The binding constants of NDS-TEMPO in the presence of salicylate and of phlorizin are identical [28]. In view of these facts, it is attractive to postulate a common binding site for inorganic anions and disulfonatostilbenes, although allosteric effects cannot be excluded completely.

The equilibrium binding data of NDS-TEMPO and the flux measurements strongly suggest that both NDS-TEMPO and substrate anions bind to a single population of sites. The Klotz plots and the Dixon plots were linear (Figs. 4 and 5) and exhibited always a competitive type of inhibition. In addition, the slope replots of the Klotz plots and of the Dixon plots were linear and the Dixon slope replot passed through the origin. These features point to a pure competition between NDS-TEMPO and substrate anions for a single binding site. A two-site binding of NDS-TEMPO should give non-linear Klotz plots and Dixon plots, while a two-site binding of substrate anions should display a mixed type inhibition of NDS-TEMPO binding and of anion transport. The slope replots from the double-reciprocal plots would be curves and the DIXON slope replot would not pass through the origin. This is in contrast to our experimental results. It should be emphasized that the substrate anion concentrations were kept low intentionally so as to avoid any interaction of substrate anions with the modifier site of the transport system.

According to our results, the equilibrium binding sites of NDS-TEMPO are identical with the NDS-TEMPO inhibitor sites. The most convincing evidence for this assumption comes from the close accordance of the equilibrium binding constants of NDS-TEMPO with the inhibitor constant of NDS-TEMPO. The equilibrium binding constants of NDS-TEMPO were between 1.0–2.0 μM, while the inhibition constants were in the range of 0.5–2.5 μM (Tables I and II). The differences between the NDS-TEMPO inhibition constants from the chloride and from the sulfate flux experiments probably are due to the different tempera-

tures at which the chloride and the sulfate flux experiments were performed. Because of the very rapid chloride exchange, the chloride and the sulfate flux experiments could not be performed at the same temperature.

The chloride and the sulfate dissociation constants from the Klotz plots are almost equal to the half-saturation constants of chloride and sulfate as obtained from the Dixon plots (Tables I and II). The sulfate dissociation constant from the Klotz plot is fairly high, but the dissociation constant and half-saturation constant of sulfate do not differ significantly. As studied so far, the binding of NDS-TEMPO in the presence of chloride and of sulfate did not show different patterns of NDS-TEMPO or substrate anion binding. The half-saturation constants of chloride, bicarbonate and sulfate were 30, 16 and 40 mM, respectively. These values are consistent with the half-saturation constants for the chloride, bicarbonate and sulfate self-exchange in red cells and red-cell ghosts [3,31,38,40–49]. The substrate anion dissociation constants supply strong evidence for the assumption that NDS-TEMPO and substrate anions compete for the transport site of the inorganic-anion-transport system and rule out a competition for the modifier site.

Note added in proof (Received June 7th, 1983)

After submission of this paper, Sitaramaya and Liebman [50] reported briefly an effect of ATP on the peak activity of phosphodiesterase similar to that presented here.

Acknowledgements

This paper is supported by the Deutsche Forschungsgemeinschaft. We are indebted to Prof. Dr. C. Albers, Prof. Dr. A. Müller-Broich, and to Prof. Dr. J. Sauer for their support of our work. We thank Dr. Mertens, Bayer A.G., Leverkusen, for supplying ANDS. We wish to thank in particular Dr. R. Knopp and Dr. E. Eibler for their helpful suggestion concerning the recording of the ESR spectra and the HPLC runs and to Dr. R. Loftus for reading and correcting the manuscript.

References

1 Deuticke, B. (1977) Rev. Physiol. Biochim. Pharmacol. 78, 1–95
2 Cabantchik, Z.I., Knauf, P. and Rothstein, A. (1978) Biochim. Biophys. Acta 515, 239–303
3 Knauf, P.A. (1979) Curr. Topics Membranes Transp. 90, 249–363
4 Knauf, P.A. and Rothstein, A. (1971) J. Gen. Physiol. 58, 190–210
5 Cabantchik, Z.I. and Rothstein, A. (1972) J. Membrane Biol. 10, 311–330
6 Cabantchik, Z.I. and Rothstein, A. (1974) J. Membrane Biol. 15, 207–226
7 Lepke, S., Fasold, H., Pring, M. and Passow, H. (1976) J. Membrane Biol. 29, 147–177
8 Ship, S., Shami, Y., Breuer, W. and Rothstein, A. (1977) J. Membrane Biol. 33, 311–324
9 Fairbanks, G., Steck, T. and Wallach, D.F.H. (1971) Biochemistry 10, 2606–2617
10 Yu, J. and Steck, T. (1975) J. Biol. Chem. 250, 9170–9175
11 Steck, T.L. (1978) J. Supramol. Struct. 8, 311–324
12 Shami, Y., Rothstein, A. and Knauf, D. (1978) Biochim. Biophys. Acta 508, 357–363
13 Barzilay, M. and Cabantchik, Z.I. (1979) Membrane Biochem. 2, 297–322
14 Fröhlich, O. and Gunn, R.B. (1980) Adv. Physiol. Sci. Vol. 6, Genetics, Structure and Function of Red Blood Cells (Hollán, S.R., Gardós, G. and Sarkadi, B., eds.), pp. 275–280, Pergamon, Oxford and Akadémiai Kiadó
15 Rao, A., Martin, P., Reithmeier, R.A.F. and Cantley, L.C. (1979) Biochemistry 18, 4505–4516
16 Dix, J.A., Verkan, A.S., Solomon, A.K. and Cantley, L.C. (1979) Nature 282, 520–522
17 Fröhlich, O. (1982) J. Membrane Biol. 65, 111–123
18 Marsh, D. (1980) in Membrane Spectroscopy (Grell, E., ed.), pp. 51–142, Springer, Heidelberg
19 McConnell, H.M. (1976) in Spin Labeling, Theory and Applications (Berliner, L.J., ed.), pp. 525–560, Academic Press, New York
20 Griffith, O.H. and Jost, P.C. (1976) in Spin Labeling, Theory and Applications (Berliner, L.J., ed.), pp. 454–523, Academic Press, New York
21 Morrisett, J.D. (1976) in Spin Labeling, Theory and Applications (Berliner, L.J., ed.), pp. 274–338, Academic Press, New York
22 Likhtenshtein, G.I. (1976) Spin Labeling, Methods in Molecular Biology, John Wiley and Sons, New York
23 Schreier, S., Polwaszek, C.F. and Smith, I.C.P. (1978) Biochem. Biophys. Acta 515, 375–436
24 Ginsburg, H., O'Connor, S.E. and Grisham, C.M. (1981) Eur. J. Biochem. 114, 533–538
25 Schnell, K.F., Flossmann, W. and Vangala, R. (1978) Pflügers Archiv 373, R. 47
26 Schnell, K.F., Flossmann, W. and Vangala, R. (1978) Hoppe-Seyler's Z. Physiol. Chem. 359, 319
27 Schnell, K.F., Käsbauer, J., Kaufmann, E. and Elbe, W. (1981) Pflügers Archiv 389, R. 47

28 Schnell, K.F., Käsbauer, J. and Kaufmann, E. (1981) Pflügers Archiv 391, R. 21
29 Bodemann, H. and Passow, H. (1972) J. Membrane Biol. 8, 1–26
30 Lepke, S. and Passow, H. (1972) Biochim. Biophys. Acta 255, 696–702
31 Schnell, K.F., Besl. E. and Manz, A. (1978) Pflügers Archiv 375, 87–95
32 Jost, P. and Griffith, O.H. (1976) Spin Labeling, Theory and Applications (Berliner, L.W., ed.), pp. 267–268, Academic Press, New York
33 Webb, L.B. (1963) Enzymes and Metabolic Inhibitors, Academic Press, New York
34 Segel, I.H. (1977) Enzyme Kinetics, John Wiley and Sons, New York
35 Gardos, G., Hoffmann, J.F. and Passow, H. (1969) Laboratory Techniques in Membrane Biophysics (Passow, H. and Stämpfli, R., eds.), pp. 9–20, Springer, Heidelberg
36 Kotyk, A. and Janáček, K. (1970) Cell Membrane Transport, pp. 151–162, Plenum Press, New York
37 Dalmark, M. and Wieth, J.O. (1972) J. Physiol. 224, 583–610
38 Schnell, K.F., Gerhardt, S. and Schöppe-Fredenburg, A. (1977) J. Membrane Biol. 30, 319–350
39 Passow, H., Fasold, H., Zaki, L., Schuhmann, B. and Lepke, S. (1975) in Biomembranes, Structure and Function (Gardos, G. and Szasz, I., eds.), Vol. 35, pp. 197–214, Hungarian Academy of Sciences, Budapest
40 Zaki, L., Fasold, H., Schuhmann, B. and Passow, H. (1975) J. Cell. Physiol. 86, 471–494
41 Gunn, R.B., Dalmark, M., Tosteson, D.C. and Wieth, J.O. (1973) J. Gen. Physiol. 57, 593–609
42 Dalmark, M. (1975) J. Physiol. (Lond.) 250, 39–64
43 Dalmark, M. (1976) Prog. Biophys. Mol. Biol. 31, 145–167
44 Brazy, P.C. and Gunn, R.B. (1976) J. Gen. Physiol. 68, 583–599
45 Brahm, J. (1977) J. Gen. Physiol. 70, 283–306
46 Passow, H., Pring, M., Legrum-Schumann, B. and Zaki, L. (1977) in Biochemistry of Membrane Transport (Semenza, G. and Carafioli, E., eds.), pp. 306–315, Springer, Heidelberg
47 Schnell, K.F. (1977) J. Membrane Biol. 37, 99–137
48 Barzilay, M. and Cabantchik, Z.I. (1979) Membrane Biochem. 2, 255–281
49 Wieth, J.O. and Brahm, H. (1980) in Membrane Transport in Erythrocytes (Lassen, U.V., Ussing, H.H. and Wieth, J.O., eds.), pp. 467–487, Munksgard, Copenhagen
50 Sitaramaya and Liebman, P.A. (1983) J. Biol. Chem. 258, 1205–1209